Shear and Dilational Surface Rheology of Oppositely Charged Polyelectrolyte/Surfactant Microgels Adsorbed at the Air−Water Interface. Influence on Foam Stability

Cécile Monteux,*,† Gerald G. Fuller,‡ and Vance Bergeron†

Laboratoire de Physique, UMR 5672, Ecole Normale Supérieure de Lyon, 46 allée d'Italie, 69364 Lyon Cedex 07, France, and Department of Chemical Engineering, Stanford University, Stanford

Received: June 11, 2004; In Final Form: July 29, 2004

Using the oscillating drop method as well as the interfacial stress rheometer (ISR), we measure the surface dilational and shear properties of adsorbed layers of oppositely charged polymer−surfactant complexes at the air−water interface. These data are compared to foam volume data measured for the corresponding solutions. We show that the shear surface moduli G' and G'' exhibit a maximum at a molar ratio of polymer monomers and surfactant in solution equal to 1. This maximum is strongly correlated to surface ellipticity measurements that indicate a strong adsorption of polymer−surfactant complexes at the air−water interface. These hydrophobic interfacial complexes generate a viscoelastic layer due to the polymer chain entanglements and hydrophobic interactions between bound surfactant. The viscous behavior of the surface layers is further characterized via creep, frequency sweep measurements, and surface aging experiments. Over a 10 h period we find that G' and G'' increase logarithmically with time, reminiscent of so-called jammed systems. Curiously, the slow evolution of G' and G'' is not reflected by significant changes in the surface tension over time, and parallel measurements for the same systems reveal that the surface complexes do not effect the surface dilational moduli, E' and E''. Finally, we observe that the foam volumes measured for the corresponding solutions also exhibit a maximum at a molar ratio of 1, indicating that the gellike layer at the interface inhibits foam drainage and bubble coalescence.

1. Introduction

Understanding interfacial rheology of adsorbed layers is of great interest for foam and emulsion stabilization. Indeed, destabilization of these systems can be due to several mechanisms such as drainage and thin-liquid film rupture both of which are known to be linked to the interfacial rheology of the dispersion interface. In particular, stress/strain relationships of adsorbed layers have been measured through shear or dilatation interfacial deformations, and subsequently related to individual foam-film stability and drainage,[1−4] as well as foam stability,[5−10] and foam rheology.[11−13] Several experimental devices can be used to measure the surface shear rheological properties of adsorbed layers at the air−water interface; knife-edge devices,[14−17] rotating disks,[18] channel flow measurements,[19] magnetic needle interfacial rheometers[20,21] and the observation of floating particle displacements.[22−25] Likewise several methods exist for measuring the dilatational surface moduli, and the choice depends on the frequency range of interest. For example, the oscillating bubble/drop method probes frequencies between 0.01 and 1 Hz, whereas a capillary wave device probes frequencies from 10 to 10^4 Hz[26,27] and surface quasi elastic light scattering enables one to investigate frequencies up to 10^6 Hz.[28] The relevant frequency range is dictated by the chemical system under investigation (e.g., surfactant, polymer), which determines the time and length scales characterizing the molecular interactions inside the adsorbed layers.

Furthermore, similar to 3D-rheology, there exist several ways of studying interfacial relaxations such as oscillatory deformations, creep (applying a constant stress and measuring the strain), or sudden strain relaxation (applying a strain and measuring stress relaxation),[29] all of which provide complementary information. Complete reviews of these techniques can be found in the literature.[30−32] Although direct comparisons between shear and dilational surface rheology for a given system has not been studied intensively,[33−35] it is rather well established that the dilational surface rheology probes the elasticity of the interface due to both intra- and intermolecular interactions, as well as the adsorption/desorption dynamics of the adsorbed molecules. All of these phenomena can influence the rupture and coalescence of thin-liquid films.[4−6] In contrast, shear surface rheology is more sensitive to interactions between the adsorbed molecules and network formation at the surface, which is known to have a pronounced influence in thin-liquid film drainage.[3]

Interfacial rheology has been investigated for more than 40 years, mainly for the study of protein layers stabilizing dispersions (i.e., foams and emulsions) in food applications.[33−41] It has been found that proteins can form highly viscoelastic layers at air−water or oil−water interfaces, with rheological characteristics that depend on pH, salinity, and concentration, as well as the intramolecular structure of the protein and its ability to unfold at the interface. For example, flexible proteins such as β-casein are characterized by a lower surface rheological moduli than globular proteins, such as β-lactoglobulin or lysozyme.[37,38,40] Surprisingly, much less attention has been paid to synthetic polymer−surfactant layers at the surface, and for the studies that exist, only a few have focused on the particular case of oppositely charged polymer surfactant mixtures.[24,25,42,43] Indeed, these systems are frequently used for many cosmetic and detergent formulations and their chemical characterization is often much easier and more complete than protein systems. The latter point is helpful when trying to understand the basic

† Ecole Normale Supérieure de Lyon.
‡ Stanford University.

10.1021/jp047462+ CCC: $27.50
Published on Web 09/22/2004

intermolecular mechanisms responsible for a given surface rheological characteristic. Hence, these synthetic systems can serve as models for the more complex protein based systems, as well as provide crucial information for optimizing commercial formulations.

In this paper we aim to measure interfacial rheological properties of oppositely charged surfactant/polyelectrolyte layers, composed of a well characterized anionic polyelectrolyte, PSS, and a cationic surfactant, C_{12}TAB, with interfacial dilatational and shear rheological measurement techniques. Furthermore, we attempt to correlate the surface rheology data to the foamability (e.g., the propensity of a system to generate foam) and the foam stability of the corresponding solutions. In previous studies,[44,45] we have studied the adsorption behavior of the same PSS/C_{12}TAB solutions used in this study with the combination of surface tension and ellipsometric measurements, as well as drainage observations from individual thin-liquid foam-films. Consistent with previous studies,[46] we observed that oppositely charged polymer/surfactant complexes strongly lower the surface tension and form surface gels at the air−water interface. Furthermore, our previous findings showed that for a 90% charged polystyrene sulfonate, two mechanisms of surface gelation behavior can occur, depending on the concentration of oppositely charged surfactant (or the ratio of the concentrations of surfactant to polymer): (1) at low surfactant concentrations ($<$cmc) (or low ratios smaller than 1), gels are due to surface precipitation of polymer−surfactant complexes; (2) at high surfactant concentrations ($\gg$cmc) or ratios between 10 and 100, gels are created during resolubilization of polymer−surfactant complexes that have precipitated out in the bulk solution. We have also found that such surface gelation is strongly influenced by the polymer molecular weight and the surfactant hydrophobicity.[45,47] These preliminary studies enable us to correlate in the present paper, the rheological properties of these adsorbed layers to their adsorption behavior. In particular, we find that the adsorbed layers formed at low surfactant/polymer ratios have very different rheological properties than those formed upon resolubilization of precipitates at higher ratios.

2. Experimental Section

2.1. Materials. The cationic surfactant, dodecyltrimethylammonium bromide, C_{12}TAB, used in this study was purchased from Aldrich and was recrystallized at least twice with a 50/50 wt % acetone/methanol mixture. Poly(styrenesulfonate) sodium salt, PSS, of molecular weight $M_W = 43300$ was purchased from Fluka and we refer to the sample as PSS 43K. The manufacturer certifies a polydispersity index, M_W/M_N of less than 1.2, which we have confirmed by MALDI-TOF mass spectroscopy (matrix-assisted laser desorption−ionization time-of-flight). Excess salt contained in PSS samples was removed through dialysis, using Spectra/Por membranes from Spectrum Laboratories Inc., with a M_W cutoff of 14000 Daltons (reorder number: 132678). Concentrated solutions of 20 g/L PSS in water were loaded in the corresponding dialysis membrane bags and dialyzed against 2 L volumes of Milli-Q water in capped polypropylene funnels. The water outside the dialysis bags was replaced several times a day for approximately 2 weeks.[48] Finally, the dialyzed solution was frozen under atmospheric pressure in liquid nitrogen before atmospheric lyophilization. Elemental analysis of 43K performed at Service Central d'Analyse of CNRS revealed that the sulfonation level of PSS is 90%. All solutions of PSS and C_{12}TAB were prepared by adding equal volumes of a solution twice the desired concentration in surfactant to a solution twice the desired concentration in PSS, using milli-Q water.

2.2. Ellipsometry. The ellipsometric data presented in this paper were discussed previously in ref 44. Using our custom-made ellipsometer, we measure the so-called "ellipticity", which is the imaginary part of the ratio of the reflection coefficients r_p/r_s of the incident beam at the air/water interface close to the Brewster angle, r_p being the reflection coefficient of the component polarized in the incidence plane, and r_s the reflection coefficient of the component polarized perpendicularly to the incident plane. The ellipticity is a function of the layer thickness at the surface and of the refractive index of the adsorbed layer. As the refractive index of our adsorbed layers is unknown, we present in this paper variations in the ellipticity values. The experimental error of the data presented is on the order of 5%, but the variations in the ellipticity observed are sufficiently large to obtain important semiquantitative information concerning the adsorbed amounts for our systems. The ellipsometry values are the values obtained after 1 h aging of the interface and are very reproducible.

2.3. Surface Tension and Surface Dilational Rheology. Surface dilational moduli measurements were performed using a modified version of the pendant drop method described earlier.[44] In this setup (see Figure 1), sinusoidal variations of a pendant drop's surface area are provoked and the surface tension as well as the surface area of the drop are measured as a function of time. First, the solution under study is injected with an airtight syringe (Hamilton-Bonaduz-Schweiz, Gastight, 1750) through a flexible silicone tubing (Tygon R3603 internal diameter 3 mm) connected to a stainless steel needle (Air tite Products Co., Inc., 14 G $\times$ 2″, 2 $\times$ 50 mm). A drop is formed at the end of the tip of the needle and kept in a sealed quartz cell (Hellma), which contains excess solution to prevent evaporation. The drop deformation is controlled through the periodic compression of the flexible silicone tube, using 2 pairs of piezoelectric disks (Murata Manufacturing Co., Ltd). These piezoelectric disks are composed of a piezoelectric ceramic plate, which has electrodes on both sides. One of the electrodes is attached to a metal plate with adhesives. Under the action of a periodic voltage applied to the two electrodes, the piezoelectric disks are distorted periodically, resulting in a periodic compression of the silicone tube. A sinusoidal voltage between 0 and 1 V is computer-generated using the Labview software (National Instruments, Version 6i) and amplified 100 times by a power amplifier (Kepco-Bipolar Operational Power supply/amplifier BOP 1000M). The piezoelectric disks are attached to a home-built support, which enables distortion of the piezoelectric disks. The drop is filmed using a CCD camera (Cohu) mounted with an optical focusing tube outfitted with a Wild pl. Fluotar objective, Heerbrugg, Switzerland, magnification by 3, 0.10 numerical aperture). The drop profile was obtained using the image analysis software Optimas 6.5, and subsequently fit numerically to the Laplace equation using a mathematical method described elsewhere,[49] which allows us to obtain the value of the surface tension (γ) as well as the drop surface area (A). From the periodic variation of γ and A with time, we deduce the dilational surface moduli as outlined below.

The Gibbs interfacial dilatational modulus is defined by the surface tension increase after a small increase in area of a surface element:

$$E = \mathrm{d}\gamma/\mathrm{d}\ln A$$

where γ is the surface tension and A isthe area of the surface element. Because the surface area of the drop is oscillated periodically, the dilatational modulus exhibits two contributions: an elastic component, E', accounting for the recoverable energy

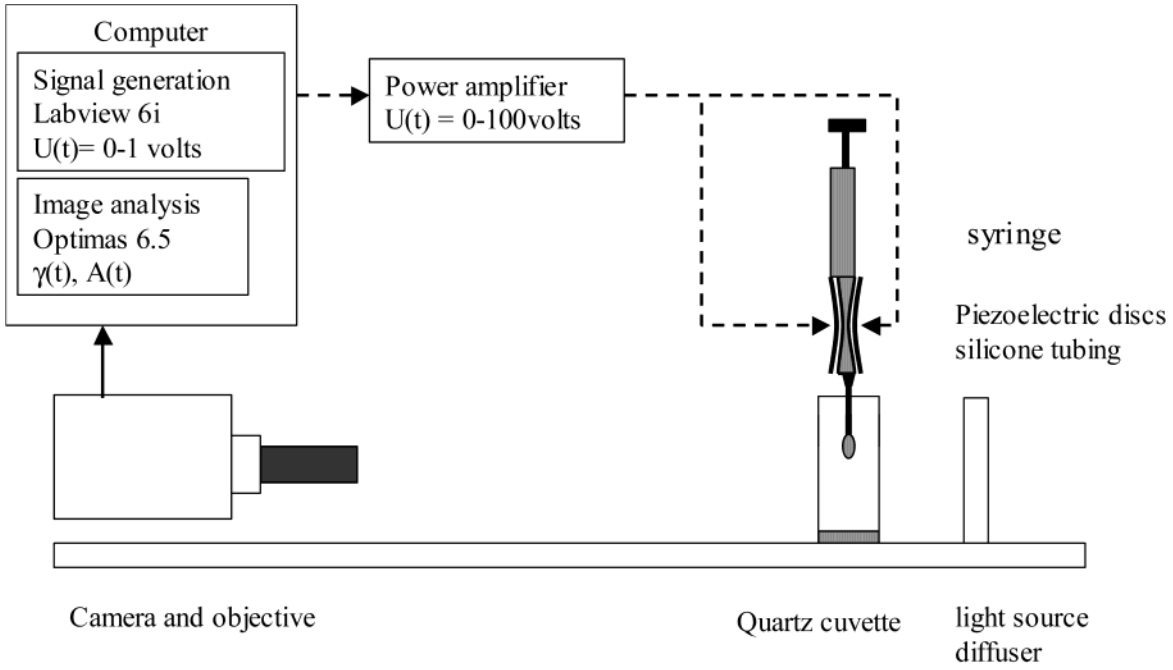

Figure 1. Experimental set up of the oscillating drop method.

stored in the interface and a loss modulus, E'', accounting for dissipation of energy through relaxation processes. The storage and loss moduli are the real and imaginary parts of the Gibbs elasticity: $\omega = E' + iE''$.

For sinusoidal oscillations of the surface area, at a frequency ω, E', and E'' are defined as follows:

$$E' = \Delta\gamma \frac{A_0}{\Delta A} \cos(\phi)$$

$$E'' = \Delta\gamma \frac{A_0}{\Delta A} \sin(\phi)$$

where $\Delta\gamma$ is the amplitude of the periodic surface tension variation, A_0 the area of the drop before oscillation or the average surface area of the drop, and ΔA the amplitude of the interfacial deformation, and Φ is the phase angle between area and surface tension curves. To determine E' and E'', the drop area and the surface tension are measured as a function of time from drop shape analysis method described above. Using the least-squares method, the data $\gamma(t)$ and $A(t)$ are fitted to the following equations to obtain the parameters $\Delta\gamma$, Φ, A_0, and ΔA:

$$A(t) = A_0 + \Delta A \cos(\omega t + \varphi_1)$$

$$\gamma(t) = \gamma_0 + \Delta\gamma \cos(\omega t + \varphi_2)$$

where γ_0 is the average surface tension and $\Phi = \varphi_1 - \varphi_2$.

With this setup, the oscillation frequency can be varied between 0.01 and 0.1 Hz. Above 0.1 Hz, our measurements are limited due to the image analysis software used. Below 0.01 Hz, the surface tension drifts slightly over several oscillation periods, leading to unreliable values of the elastic moduli. The deformation $\Delta A/A_0$ is set equal to 3% to avoid nonlinear effects, and we have confirmed that the deformation of the drop varies linearly with the voltage applied to the piezoelectric disks. A calibration of the piezoelectric disks is required to obtain the voltage needed for a desired drop deformation. The silicone tubing and syringe are left overnight in ethanol prior to any measurement, and then rinsed tens of times with both ethanol and deionized water.

Experimentally, the drop surface tension is followed over 1 h, and then the drop is periodically deformed during 2 min. Thus, the moduli presented are those measured after 1 h aging of the interface. As explained in ref 44, values of the surface tension as well as the dilational surface moduli are measured while the system is not necessary at equilibrium. Indeed, absolute equilibrium with such complex systems of macromolecular species is questionable. However, the evolution of the surface tension after 1 h was minor compared to differences between samples and all measurements were very reproducible and performed at room temperature.

2.4. Surface Shear Rheology: Interfacial Stress Rheometer Apparatus. Surface shear rheology of the layers formed by surfactant−polymer complexes is studied with an interfacial stress rheometer, which is described in detail in the references from Brooks et al.[20] In this set up, a Teflon-coated magnetic needle is kept floating at the air−water interface inside a glass channel and is subjected to an oscillatory magnetic force generated by a pair of Helmoltz coils. The resulting motion of the needle was detected using an optical microscope and a photodiode array that detects the shadow of the needle behind the light source. The oscillating magnetic field induces a sinusoidal motion of the rod at the same frequency but different in phase. The rod's displacement divided by the distance between the needle and the glass wall defines the surface strain. From the time dependent surface strain response to the applied surface stress created by the magnetic field, one is able to determine the phase lag, δ, between the stress and the strain, as well as the ratio of their amplitudes, AR. From AR and δ, and after calibration of the setup, one is able to measure the complex shear surface modulus $G^*(\omega)$, which is a complex number defined as the sum of two contributions: $G^* = G' + iG''$, where G' represents the elastic properties and G'' is the loss modulus and describes the viscous behavior.

For all the solutions investigated, the interfacial shear moduli exhibit no dependency on the strain amplitude over strains ranging from 0.001 to 0.03, indicating that we conducted measurements in the linear viscoelastic regime (see Figure 2). In the case of the frequency sweeps experiments, the frequency ranges from 0.05 to 0.5 Hz (0.34 to 3.4 rad/s).

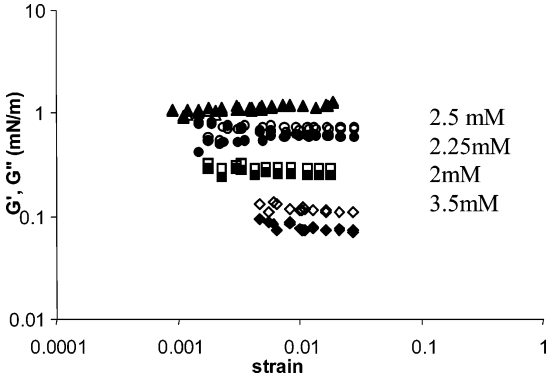

Figure 2. G' and G'' (closed and open symbols, respectively) as a function of strain for different C_{12}TAB/PSS solutions for 2, 2.25, 2.5, and 3.5 mM (corresponding to [C_{12}TAB]/[PSS] ratios of 0.83, 0.93, 1.04, and 1.46, respectively). G' and G'' are independent of the strain, illustrating that the experiments are performed in the linear viscoelastic regime.

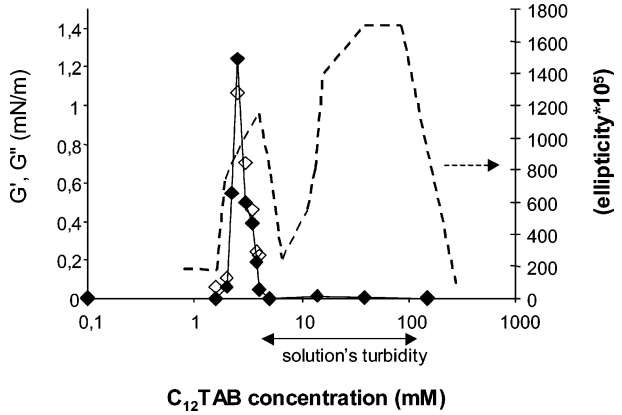

Figure 3. Storage and loss surface shear moduli, G' and G'' (closed and open symbols, respectively) and ellipticity as a function of C_{12}TAB concentration for solutions containing 2.4 mM PSS. The values are taken after 1 h aging of the interface. The frequency is 0.1465 Hz. It should be noted that the same dependence of G', G'' with the surfactant concentration is observed for all the frequencies.

2.5. Foaming Power and Foam Stability. Foaming power measurements are performed with a modified Ross−Miles test. Twenty milliliter syringes are filled with the solution of interest. The liquid contained in the syringe is then injected into a 100 mL graduated cylinder containing 10 mL of the same injection fluid at a constant speed, with the help of a motor. The impacting fluid inside the cylinder creates a foam, the volume of which is measured visually, using the graduations on the cylinder. The decay of the foam, due to foam drainage and bubble coalescence, is followed over time for 30 min.

3. Results

To characterize the mechanical properties of the C_{12}TAB/PSS complexes at the air−water interface and relate them to our previous adsorption studies, we have studied the shear and dilatational surface rheology of C_{12}TAB/PSS solutions as a function of the C_{12}TAB concentration (from 0.05 to 400 mM) for a concentration of PSS monomers equal to 2.4 mM (i.e., 0.5 g/L of polymer).

3.1. Surface Shear Rheology. In Figure 3, we present the values of G' and G'', storage and loss shear surface moduli, measured with the interfacial stress rheometer at a frequency of 0.1465 Hz for C_{12}TAB/2.4 mM PSS as a function of C_{12}TAB concentration. The data are portrayed by open and filled diamonds in the figure. A solid line is drawn through the data to provide a guide. The dotted line in Figure 3 represents previous ellipsometry data obtained for the same system and is fully discussed in ref 44. Briefly, the complex behavior of the ellipticity as the surfactant concentration is increased is explained as follows. The ellipticity first increases with C_{12}TAB concentration as C_{12}TAB binds to PSS in complexes that become highly surface active. At this stage, we also observe that the thin-liquid foam films formed from these solutions (2.4−4 mM C_{12}TAB) contain aggregates and undergo a very slow drainage, the latter indicating a high surface viscosity. This is interpreted by the formation of a surface gel (i.e., a semisolid layer at the air−water interface). At higher surfactant concentration, the PSS molecules start to become saturated with surfactant, the complexes become insoluble and desorb partially from the air/water interface. Consequently, most of them precipitate out of solution, resulting in a dramatic fall in ellipticity around 9 mM C_{12}TAB. Finally, when the C_{12}TAB concentration is further increased, these precipitates partially ressolubilize by the association of a second layer of surfactant to the first layer bound to the PSS backbone. These newly charged complexes are surface active and adsorb at the air−water interface, producing a second rise of ellipticity, which peaks near 50 mM C_{12}TAB. For concentrations of C_{12}TAB reaching 20 times the cmc (i.e., 280 mM C_{12}TAB), C_{12}TAB/PSS complexes become completely soluble in water, and deplete the surface, leaving the interface saturated with a monolayer of surfactant.

3.1.1. Influence of the Surfactant Concentration (or Surfactant/Polymer Molar Ratio). It can be seen from Figure 3 that G' and G'' have very close values over the entire range of surfactant concentrations investigated. Both G' and G'' are nearly zero up to a surfactant concentration of 1.45 mM. At this point there is a sharp rise to a maximum value at 2.43 mM C_{12}TAB, where $G' = 1.24$ mN/m and $G'' = 1.12$ mN/m. Following this maximum is a rapid decrease and return to zero above 5 mM of surfactant. Most noteworthy, the maximum in the shear moduli occurs inside the zone of maximum ellipticity corresponding to a molar ratio [C_{12}TAB]/[PSS] near unity, where the molar concentration of PSS monomers equals the concentration of C_{12}TAB molecules. This result is consistent with the formation of a concentrated gellike layer at the air−water interface composed of highly hydrophobic PSS/C_{12}TAB complexes, at their limit of solubility. The high surface concentration enable interactions between PSS/C_{12}TAB complexes−chain entanglements as well as hydrophobic interactions between surfactant tails probably explain the observed viscoelastic behavior of the layer under this shear deformation. In particular, for the 2.5 mM C_{12}TAB/PSS solution, corresponding to a molar ratio of 1, it can be seen that G' is higher than G'', which is characteristic for the adsorption of an elastic layer. It can be seen that the peak in the shear moduli is narrower than the first peak in ellipticity, and the value of G' and G'' already return to 0.22 mN/m for a 4 mM C_{12}TAB/PSS solution. This is surprising, as a high surface viscosity was expected from the drainage studies presented in our previous study.[44] Indeed, the foam-films drawn from the 4 mM solution contained the most numerous aggregates and the longest drainage times, which was interpreted as a sign of high surface viscosity and the formation of a semisolid layer at the air−water interface. These complementary rheological data suggest that the surface viscosity is not the only parameter responsible for the slow film drainage. In addition to the surface viscosity, the presence of the aggregates bridging the film interfaces apparently provides substantial resistance to flow out of the films.

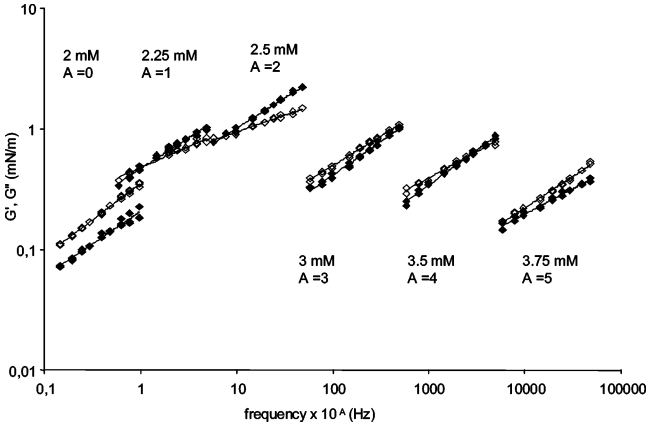

Figure 4. Logarithmic frequency dependence of G', G'' (closed and open symbols, respectively) for C_{12}TAB/PSS solutions of 6 different C_{12}TAB concentrations.

Between 4 and 10 mM C_{12}TAB, corresponding to the partial desorption and precipitation of insoluble PSS/C_{12}TAB complexes, we measure low surface moduli, as expected from our adsorption studies. More unexpectedly, we find that the shear surface moduli are equal to zero between 10 and 100 mM surfactant, concentrations corresponding to the second maximum in ellipticity, where ellipsometry measurements indicate that ressolubilized surfactant−polymer precipitates adsorb strongly at the air−water interface. In our previous study, based on neutron reflectivity results from Taylor et al.,[50] we have attributed this second peak in ellipticity to the formation of a structured layer of PSS and C_{12}TAB, where the C_{12}TAB molecules form a monolayer at the air−water interface and PSS chains are located in a subsurface layer bound to C_{12}TAB bilayers or micelles. The absence of a peak in surface shear moduli at this point indicates that this subsurface layer can be viewed as rather mobile and not highly entangled with the surface, thus offering little resistance to interfacial flows.

3.1.2. Frequency Spectrum: Oscillations and Creep Experiments. Figure 4 presents the values of G' and G'' as a function of the frequency ω of the sinusoidal oscillations for surfactant concentrations between 2 and 3.75 mM. It can be seen that G' and G'' are nearly equal and vary as a power of the frequency, i.e., $G' = \omega^{n'}$ and $G'' = \omega^{n''}$, n' and n'' being nearly equal for all the surfactant concentrations and ranging between 0.3 and 0.6. Similar exponents have been found by Brooks et al.[20] for a system composed of an insoluble surfactant mixed with rigid polymer molecules. In another study, exponents of 0.5 over several orders of magnitude of the frequency were attributed to the formation of a surface gel[51] in reference to theoretical works on 3D-chemical gelation.[52] In our case the range of frequency only spreads over 1 order of magnitude, which is not sufficient to draw such a conclusion. More simply, it can be said that an exponent of $n = 0$ for $G(\omega) = [(G'(\omega))\Sigma + (G''(\omega))\Sigma]\alpha\omega^n$ is characteristic for purely elastic layers such as elastomers, whereas $n = 1$ is characteristic for purely viscous Newtonian liquids.[53] As such, a typical interpretation is that the lower the exponent of the frequency dependence, the more solidlike the material is. In our case, the exponents n' and n'' as well as n being between these two extremes, we conclude that our adsorbed layers are a viscoelastic semisolid, whose rigidity results from chain entanglements and hydrophobic interactions.

To probe slower relaxation mechanisms, we have performed creep experiments where a sudden and constant shear stress is applied to the surface, and the displacement of the needle, related to a strain, is followed with time. From this experiment we can plot the creep compliance (the strain divided by the constant stress) as a function of time (Figure 5a) when a stress of 0.0028 mN/m is applied to the interface at $t = 0$ s. Physically, the compliance is a measure of how easily the system flows under a given stress. As indicated by Macosko,[54] the response can be fit to a model that incorporates 2 time scales:

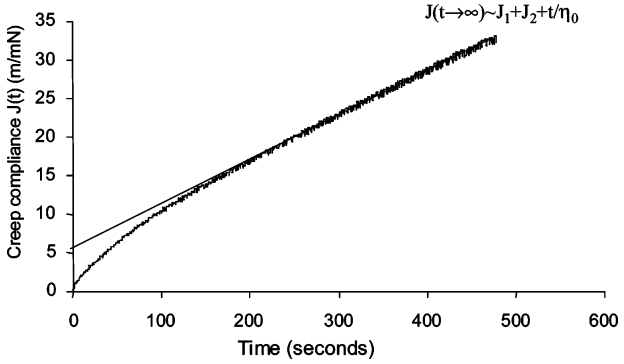

Figure 5. $J(t)$, creep compliance as a function of time for a 2.5 mM C_{12}TAB/2.4 mM PSS solution.

$$J(t) = \frac{t}{\eta_0} + J_1(1 - e^{-(t/\tau_1)}) + J_2(1 - e^{-(t/\tau_2)})$$

where η_0 is the shear viscosity in the limit of low shear rates and J_n is the compliance with the associated time constant τ_n. This model corresponds to two Voigt elements in series (i.e., a dashpot and a spring in parallel) together in series with a dashpot. The two Voigt elements describe viscoelastic solids with two different characteristic length and time scales, and the dashpot corresponds to the long-time viscous dissipation of the adsorbed layer. From the curve fit seen in Figure 5, we find $\eta_0 = 18.3$ mN/m, $J_1 = 4.3$ m/mN, $\tau_1 = \eta_1 J_1 = 92$ s, $J_2 = 1$, and $\tau_2 = 5.2$ s. The characteristic times, τ_1 and τ_2, that we measure are much smaller than those presented in other studies. For example, Brooks[55] and Nauman[56,57] have found characteristic times of 100 and 1500 s for adsorbed layers composed of lipopolymers composed of PEO chains and UV-polymerized elastomeric networks, respectively. This comparison confirms that our 2.5 mM C_{12}TAB/PSS layers probably have the structure of a soft physical gel with connections made of simple entanglements between polymer chains, and hydrophobic bonds via surfactant tails shared between polymer chains, which have lower cohesive energies than covalent links or hydrogen bonds as in the case of Nauman or Brooks. At long times, or zero frequency, the chains disentangle and the hydrophobic links break, resulting in a Newtonian-like behavior.

3.2. Surface Dilational Rheology. Figure 6 presents the values of the dilational storage and loss surface moduli (full and open triangles, respectively) obtained using the oscillationg drop method as a function of the concentration of C_{12}TAB. The frequency of oscillations is 0.05 Hz and the percentage of deformation is 3%. First, it should be noted that for pure C_{12}TAB solutions (not shown), E' and E'' remain below 4 mN/m for all the surfactant concentrations. When 2.4 mM background PSS is added to the surfactant solutions, the values of E' increase to a maximum value comprised between 20 and 35 mN/m at 1.95 mM C_{12}TAB and then return to 5 mN/m for a concentration of 2.43−39 mM C_{12}TAB. It is important to note that this maximum in the surface dilatational moduli is measured between 1 and 2 mM of C_{12}TAB, where no surface microgels were observed in the corresponding thin-liquid films and at a lower surfactant concentration than the first peak in ellipticity. Moreover, the maximum in the dilational moduli occurs over a very narrow range of surfactant concentrations. This phenomenon as well

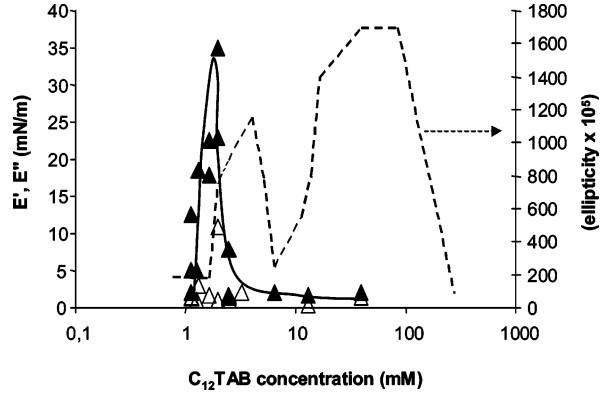

Figure 6. Storage and loss surface dilational moduli E' and E'' (closed and open symbols, respectively) and ellipticity as a function of C_{12}TAB concentration for solutions containing 2.4 mM PSS. The values are taken after 1 h aging of the interface. The frequency is 0.05 Hz. The foam films corresponding to the 2.4 mM solution contains small aggregates whereas for the 4 mM solutions, the film contains large aggregates and is highly deformed.

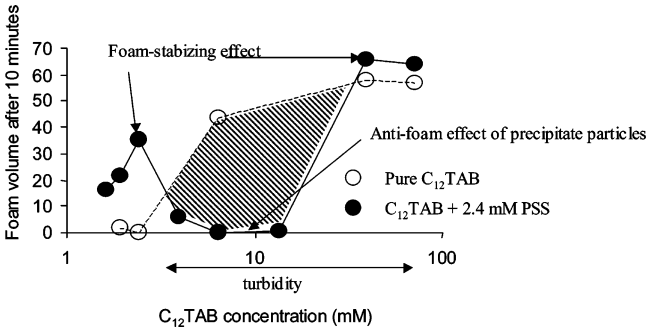

Figure 7. Foam volume measured with the normalized Ross−Miles test as a function of C_{12}TAB concentration, for pure C_{12}TAB solutions and for C_{12}TAB/2.4 mM PSS solutions. At low surfactant concentrations and above 38 mM, C_{12}TAB/PSS complexes behave as foaming agent. Between 5 and 38 mM, C_{12}TAB/PSS complexes precipitate into hydrophobic particules that behave as antifoam.

as the complexity of the investigated system has rendered the precise determination of E' and E'' difficult. Although we have performed a high number of experiments, an important inconsistency is observed in the experimental data. Although the absolute values of the moduli are somewhat scattered, we are confident concerning the position of the maximum in the moduli as a function of the surfactant concentration, and we have confirmed that after 3 mM of surfactant, the surface dilational moduli returns to significantly lower values (see Figure 6). Comparing this result with thin-liquid films studies from ref 44, shows that the maximum in dilational moduli occurs before 2 mM surfactant, where the thin liquid films do not contain any aggregates and undergo symmetric relatively fast drainage (approximately minutes). On the contrary, for solutions between 2.4 and 4 mM surfactant, the dilational surface moduli are zero although the corresponding foam films contain numerous aggregates, and undergo extremely slow drainage (hours).

3.3. Foam Stability. Figure 7 represents the foam volume remaining 10 min after generation by our modified Ross−Miles apparatus, as a function of C_{12}TAB concentration for pure C_{12}TAB solutions, as well as with solutions having 2.4 mM background PSS. For pure surfactant solutions, the foam volume increases monotonically from zero to 60 mL when the concentration of surfactant is raised from 1 to 90 mM (6 times the CMC). After addition of PSS to the surfactant solutions, the foam volume is increased from zero up to 40 mL for surfactant concentrations between 1 and 2.4 mM. The maximum in the foam volume is measured for a molar ratio of 1, where the concentration of C_{12}TAB molecules equals the concentration of PSS monomers, similar to what has been found with other systems of oppositely charged polymer−surfactants.[58] More generally, it has been observed by several authors that the foaminess of polymer solutions as well as partially miscible ternary systems is often a maximum at their limit of phase separation.[59,60] In our case, when the molar ratio is equal to 1, polymer−surfactant complexes are at their limit of solubility and adsorb at the air−water interface in a viscoelastic concentrated layer, which is effective at lowering the rate of foam drainage and coalescence. We should add that the volume of foam created right after injection is the same for pure as well PSS containing solutions. Thus, in this concentration range the added PSS acts as a foam stabilizing agent.

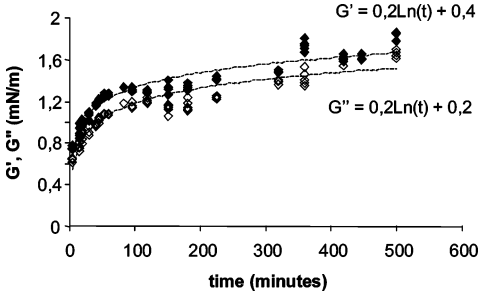

Figure 8. G' and G'' of a 2.5 mM C_{12}TAB/2.4 mM PSS solution as a function of time (closed and open symbols, respectively). This solution corresponds to the maximum in G', G'' from Figure 2.

Between 8 and 20 mM surfactant, where C_{12}TAB/PSS precipitates out of solution, the foam volume created by mixed PSS/surfactant solutions returns to zero, whereas the pure surfactant solutions attain their maximum. For the PSS containing solutions, two phenomena are likely responsible for this poor foaming behavior: (1) most of the surfactant is bound to the polymer complexes that have precipitated out of solution, leaving insufficient amounts for high foam stability, (2) the polymer−surfactant precipitates act as hydrophobic antifoam particles, which can provoke foam collapse.[61] After 38 mM surfactant, corresponding to the ressolubilization of C_{12}TAB/PSS complexes, the foam volume of C_{12}TAB/PSS solutions increases up to 70 mL, which is slightly higher than the corresponding pure surfactant solutions. Therefore we have seen that between 1 and 2.43 mM C_{12}TAB and between 38 and 100 mM C_{12}TAB polymer/surfactant complexes behave as a foaming agent, whereas, on the contrary, between 8 and 20 mM, surfactant−polymer complexes are insoluble and induce foam collapse.

3.4. Aging of the 2.5 mM C_{12}TAB/2.4 mM PSS Solution. Owing to the maximum in the surface shear viscosity and foam stability at 2.5 mM C12TAB with 2.4 mM added PSS (i.e., molar ratio of approximately 1) we have further characterized this system and its time evolution over several hours. Figure 8 shows the evolution of the shear surface moduli G' and G'' as a function of time during a 10 h period, and Figure 9 presents the surface tension as a function of time for 30 min. From Figure 8 it can be seen that G' and G'' increase logarithmically with time; this is illustrated by the lines corresponding to the best fits of G', $G'' = a \ln(t/\tau)$. This behavior is similar to what is observed during aging of jammed systems, such as colloidal gels, or polymer glasses and indicates that slow relaxation mechanisms take place at the air−water interface of the 2.5 mM C_{12}TAB/2.4 mM PSS solution. It can also be noted that G' remains higher than G'' throughout the entire experiment, which is characteristic for elastic systems such as gels. Surpris-

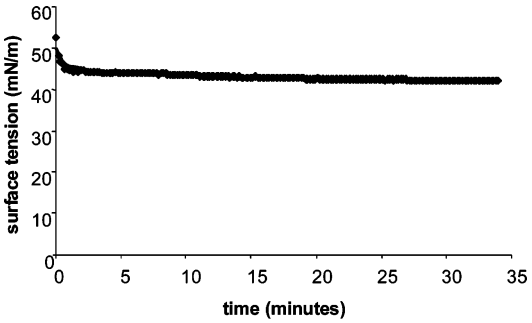

Figure 9. Surface tension of a 2.5 mM C_{12}TAB/2.4 mM PSS solution (corresponding-to-a ratio of surfactant molecules to PSS monomers equal to 1) as a function of time. After 45 s, the surface tension is already 45 mN/m.

TABLE 1: Comparison of Dilational and Shear Surface Moduli Obtained with Various Systems: Flexible and Globular Proteins, Pure Polymers or Pure Surfactants, Polymer−Surfactant Complexes

system	E' (mN/m)	G'(mN/m)	ref
lysozyme (hexadecan/water)	30 to 75	0 to 20	33
lysozyme (chloroform/water)	0 to 100		61
BSA (air/water)	0 to 60		41
eicosanol/rigid polymer		0.01 to 10	20
PEO lipo-polymers (air/water)		0.1 to 4	56, 57
C_{12}TAB/PAMPS complexes (air/water)	0 to 50		42
our C_{12}TAB/PSS complexes (air/water)	0 to 40	0.01 to 1.5	
β-casein (air/water)	0 to 30	0.01 to 2	40, 51
β-casein (hexadecan/water)	1 to 6	0.1 to 0.3	33
pure polymers (PVP, PEO, EHEC)	0 to 10		62−65
pure surfactants	0 to 5	0.01 to 0.1	42, 20

[a] For both G' and E', the investigated frequencies range from 0.01 to 2 Hz.

ingly, Figure 9 shows that the surface tension decreases much more rapidly. Indeed, the surface tension is 45 mN/m after 5 min and does not decrease significantly further over the following 30 min. This behavior indicates that the structural rearrangements that occur inside the adsorbed layers of PSS and C_{12}TAB complexes lead to the logarithmic increase of G' and G'' but do not strongly influence the surface tension. That is, it appears that material adsorbs relatively quickly to the interface and takes a much longer time to rearrange.

4. Discussion

4.1. Comparison between C_{12}TAB/PSS Interfacial Complexes and Other Systems. To formulate qualitative information concerning the structure of the PSS/C_{12}TAB layers at the air−water interface, it is useful to compare the absolute values of G' and G'' (between zero to 1.5mN/m) and E' and E'' (between 0 and 40 mN/m) to the values obtained with other systems using shear and dilational rheology. The results from the literature are summarized in Table 1. We have chosen data obtained with the same experimental techniques (ISR and oscillating drop for shear and dilational surface rheology, respectively). Globular proteins such as lysozyme or BSA are characterized by E' between 0 and 100 mN/m and G' between 0 and 20 mN/m. Flexible proteins such as β-casein are characterized by dilational moduli between 0 and 30 mN/m and shear moduli between 0 and 2 mN/m, respectively. For solutions of pure hydrosoluble polymers[62−65] or pure surfactants, much lower values of the surface dilational moduli are reported, E' ranges between 0 and 10 mN/m, and values below 0.1 mN/m are reported for G' in the case of eicosanol, an insoluble surfactant. The values of G' and E' we report for our C_{12}TAB/PSS complexes are thus much higher than those obtained for pure surfactant or pure polymer solutions and are intermediate between those measured for flexible and globular proteins. Last, we specifically note Naumans's studies on lipopolymers, whereslightly higher shear surface moduli than in the present study were found. We also report the results obtained with the oscillating pendant drop for a similar system of oppositely charged polymer−surfactant complexes. Ritacco et al.[43] found for mixtures of PAMPS and C_{12}TAB values of dilational moduli between 5 and 50 mN/m at frequencies of 0.05 Hz, which is similar to the present case.

These results show that the dilational and shear surface moduli are closely related to the kind of intermolecular and intramolecular interactions involved in the adsorbed layers. For example, globular proteins such as lysozyme or BSA are known to form strong intermolecular interactions through hydrogen bonds and disulfid covalent bridges and exhibit the highest shear and dilational moduli. On the contrary, β-casein, which is a much more flexible molecule because of weaker intermolecular interactions, is usually represented as a natural amphiphilic copolymer with a configuration close to the random coil and exhibits much lower surface moduli. In the case of Naumann's lipopolymer, the authors show that hydrogen bonds are formed between PEO chains, explaining the intermediate values of G' and G'' between those of β-casein and lysozyme. In the case of the eicosanol/PcPS system, the structure of this hairy-rod rigid polymer as well as its ability to undergo isotropic/nematic transition explains the high values of G'. For pure surfactant solutions only hydrophobic interactions between surfactant molecules provide surface viscoelasticity, whereas purely polymeric adsorbed layers are viscoelastic because of chain entanglements. Our C_{12}TAB/PSS complexes combine chain entanglements as well as hydrophobic interactions, but the absence of stronger bonds such as disulfide bridges or hydrogen bonds explains why their behavior is intermediate between flexible and globular proteins.

We should add that in the case of proteins (BSA), it has been reported that the highest surface shear moduli was measured at a pH close to their isoelectric point, when the net charge of the protein is close to zero and therefore its hydrophobicity is maximal.[37] Also, in the case of oppositely charged polymer−surfactant systems, the qualitative suface rheological studies from Regismond et al.[24,25] have shown that surface viscoelasticity was measured at the limit of solubility of the complexes, close to the precipitation zone. Similarly, in our case, the maximum shear surface moduli of our PSS/C_{12}TAB solutions is observed for a molar ratio of unity, when PSS chains are nearly saturated with C_{12}TAB molecules (i.e., the PSS/C_{12}TAB complexes are most hydrophobic, just before bulk precipitation).

4.2. Comparison between Shear and Dilational Surface Rheology. From Figures 3 and 6, we have seen that the surface shear moduli reach a maximum within the concentration range that shows a maximum in ellipticity. This has been attributed to the adsorption of highly hydrophobic surfactant−polymer complexes in a viscoelastic concentrated layer where connectivity is due to chain entanglement as well as hydrophobic links between surfactant chains. On the contrary, the occurrence of the peak of the dilational moduli at lower surfactant concentrations than the shear moduli remains unexplained.

One possible explanation for this behavior is that PSS/C_{12}TAB complexes inhibit surface tension gradients because they diffuse to the interface faster than the rate of deformation of the interface. In section 3.4, we have shown that the dynamics of the surface tension for the 2.5 mM solution is relatively fast—in nearly 45 s, the surface tension decreases from 52 to 45 mN/m, which represents 70% of the amplitude of the surface tension

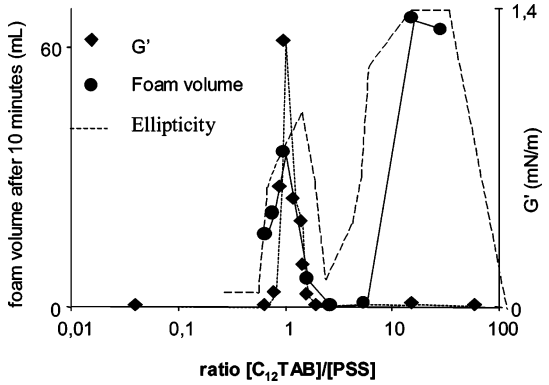

Figure 10. Foam volume, G', and ellipticity as a function of C_{12}TAB to PSS molar ratio. The data points are the same as in Figures 3 and 7. To obtain the surfactant/polyelectrolyte ratio, the surfactant concentration is divided by 2.4 mM, the concentration in PSS monomers.

decrease after 30 min. Therefore the characteristic frequency for diffusional exchange is around 0.02 s^{-1}, which is on the same order as the frequency of the oscillations. Thus 0.05 Hz is a frequency where diffusional exchange PSS/C_{12}TAB may prevent the buildup of high surface tension gradients. However, because the complexes are very hydrophobic, it remains surprising that these layers are so compressible. Hence the intrinsic rigidity of our C_{12}TAB/PSS complexes must be relatively low. We note that the maximum in the dilational moduli is obtained for a C_{12}TAB concentration between 1 and 2 mM, where the characteristic time for the decrease of the surface tension is of the order of 1000 s. To ensure a negligible contribution from diffusion of the adsorbing complexes, we would need to investigate frequencies below 0.001 Hz; however, we have had difficulty in obtaining reliable values using our current experimental setup.

An alternative consideration of these results is to assume that the dilation moduli that we present here are not directly comparable to the shear surface moduli, as was shown by Freer et al.[33] Their study is dedicated to the comparison of shear and dilational rheology of β-casein and lysozyme using the oscillating bubble method (instead of the drop) and the ISR. Knowing that the dilational elastic modulus E' is composed of a static and a dynamic component, E_∞ and $\delta E'$, respectively, the authors show that the dynamic modulus $\delta E'$, representing the recoverable dilational storage modulus is the only variable to be compared with G'. The authors measure E_∞ by imposing a sudden compression to the bubble and measuring the relaxation of the surface tension with time. E_∞, equivalent to a zero frequency modulus, is the difference between the surface tension immediately after the compression and the surface tension measured after relaxation, divided by the percentage of deformation. From their measurement of E_∞ the authors deduce $\delta E'$ as the difference between E' and E_∞. The authors show that although E' and G' are not correlated, $\delta E'$ and G' follow the same evolution. This interesting work shows that direct comparison between E' and G' is not trivial. We have attempted to measure E_∞ to evaluate $\delta E'$, but the variation of the surface tension after compression of the drop was smaller than 0.5 mN/m, which is close to the precision of our measurements, and thus we are able to adequately determine $\delta E'$.

As mentioned previously, another difficulty in interpreting dilatational surface rheology measurements is the coupled influence of the rigidity of the layer and the kinetics of desorption/adsorption of adsorbed molecules during compression/extension of the interface. To eliminate the diffusional component, Freer et al.[33] rinse the solution around their bubbles, with pure water. All reversibly adsorbed molecules are rinsed away with the solution and the following oscillation of the bubble only probes the remaining irreversibly adsorbed molecules. Experimental work is under way with our system to see if this method can help further to understand our surface layers.

4.3. Correlation between Surface Rheology and Foam Stability. We have seen that there exist two zones of surfactant concentrations where the foam volume measured with PSS/C_{12}TAB solutions is higher than the foam volume for pure surfactant (or pure PSS) solutions. Figure 10 represents the evolution of the foam volume, G', and ellipticity as a function of the C_{12}TAB/PSS molar ratio. It can be seen that the first peak in the foam volume occurs for the same molar ratio of 1 as the peaks in G' and in ellipticity. This result shows that for the polymer/surfactant systems studied here, the foam stability is strongly correlated to shear surface moduli. Several studies have shown that dilational surface moduli can be more important for foam stability than shear surface moduli; however, these studies mainly concern pure surfactant solutions,[4] for which shear surface moduli are very low because of the lack of connectivity between molecules in comparison to polymeric systems. With these simpler systems, foam stabilization is more strongly dependent on surface tension gradient mechanisms. In the literature, direct comparisons between foam stability and surface rheology (shear and dilational) for systems having high shear surface viscosities are scarce. Batthacharyya and Ritacco[42,43] compare the dilational moduli obtained with the oscillating drop method to foam stability for a system of 25% PAMPS and C_{12}TAB, similar to our PSS/C_{12}TAB system. From their data the authors conclude that foam stability is influenced by high surface elasticities but the experimental error prevents

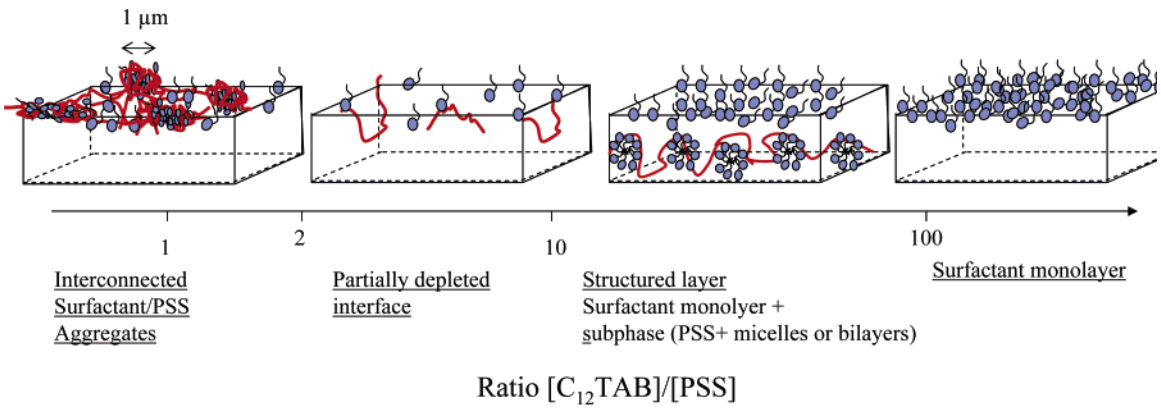

Figure 11. Possible structures of the PSS/C_{12}TAB adsorbed layers at the air−water interface as a function of the C_{12}TAB/PSS molar ratio.

us from determining an eventual correlation between the peak in the dilational surface moduli and a maximum in foam volume.

In this study, at surfactant/polymer ratios between 10 and 30, where ellipsometry measurements reveal adsorption of newly charged complexes, the foam stability exhibits a second peak but we measure no significant shear surface moduli in this concentration region. In this case, the foam volume is only slightly increased in comparison to pure surfactant solutions and we speculate that additional repulsive forces within the foam films due to the subsurface layers are responsible for this increase.

5. Conclusion

We have measured the surface rheological properties of C_{12}TAB/PSS solutions as a function of the concentration of C_{12}TAB or the molar ratio of C_{12}TAB/PSS and compared these results to previous ellipsometric results, as well as foam volume measurements. Figure 11 presents the possible structures of our C_{12}TAB/PSS adsorbed layers as a function of the molar ratio of surfactant to polymer concentrations. We have seen that for a molar ratio equal to unity between polymer monomers and surfactant molecules, there is a clear correlation between the peaks in ellipticity, the shear surface moduli, and the foam volume. For a molar ratio of 1, the hydrophobicity of PSS complexes appears to be optimized, resulting in the adsorption of a concentrated layer at the air−water interface, as revealed by ellipsometry. The high surface concentration enables strong interactions between adsorbed C_{12}TAB/PSS complexes. As a result, the viscoelastic character of the layer is due to chain entanglements and hydrophobic links between surfactant tails. Moreover, at this point we also find low exponents for the frequency dependence of G' and G'' (between 0.3 and 0.6), similar absolute values of G' and G'' compared to the literature concerning globular and flexible proteins, as well as the fact that $G' > G'$. Taken together, these findings enable us to conclude that these surface layers behave like a semisolid material or a soft surface gel. Furthermore, the slow logarithmic evolution of G' and G'' over long periods of time, similar to jammed systems, confirms the image of a surface gel, which undergoes very slow molecular rearrangements over long periods of time. The maximum in the foam volume at this ratio is due to this gellike adsorbed layer at the air−water interface, which slows down thin-film drainage and inhibits bubble coalescence. The low dilational moduli we observe at ratios close to 1 may be due to the fact that surfactant−polymer complexes diffuse to the interface faster than the rate of deformation of the interface, which inhibits high surface tension gradients.

At higher ratios (between 2 and 10), surfactant−polyelectrolyte complexes precipitate out of the supernatant solution, leaving it depleted of surfactants and polymer. Therefore there are insufficient amounts of surfactant in the solution for foam stability. Moreover, the hydrophobic precipitates can act as antifoam particles and provoke foam collapse. The partial desorption of PSS/C_{12}TAB complexes from the interface results in low shear surface moduli.

At ratios between 10 and 30, ressolubilized PSS−C_{12}TAB complexes adsorb strongly to the air−water interface, but this is not accompanied by a second peak in the shear surface moduli. Here the formation of a mobile structured layer composed of a surfactant monolayer and a sublayer composed of PSS chains and surfactant micelles or bilayers is weakly linked to the surface and provide little resistance to interfacial flows. This sublayer may be responsible to the slight increase in foam stability observed at these high molar ratios, due to additional repulsive force between the interfaces.

Acknowledgment. This work was supported by Rhodia Specialty Chemicals, as well as the CNRS (Centre National de la Recherche Scientifique). First we thank Jay Anseth from Stanford University, for his experimental help with the ISR experiments. We also thank Eric Freyssingeas and J. F. Palierne from ENS Lyon as well as Clay Radke and E. Freer from Berkeley University for helpful discussions concerning the surface rheology data. A-F. Leron and P. De Lanty from Rhodia are also acknowledged for their kind advice concerning the Ross−Miles experiment, as well as R. Miller from Max-Planck Institute-Berlin, who kindly gave us the piezoelectric disks.

References and Notes

(1) Cohen-Addad, S.; Di Meglio, J. M. Stabilization of aqueous foam by hydrosoluble Polymers. Role of Polymer−surfactant interactions. *Langmuir* **1994**, *10*, 773−778.

(2) Koehler, S.; Himgenfeldt, Weeks, E. R.; Stone, H. A. Drainage of single Plateau borders: Direct observation of rigid and mobile interfaces. *Phys. Rev. Lett. E* **2002**, *66*, 040601 1−4.

(3) Joye, J. L.; Miller, C. A.; Hirasaki, G. J. Dimple formation and Behavior during axisymmetrical Foam Film Drainage. *Langmuir* **1992**, *8*, 3083−3092.

(4) Fruhner, H.; Wantke, K. D.; Lukenheimer, K. Relationship between surface dilational properties and foam stability. *Colloids Surf. A* **1999**, *162*, 193−202.

(5) Wasan, D. T.; Nikolov, A. D.; Lobo, L. A.; Koczo, K.; Edwards, D. A. Foams, thin films and surface rheological properties. *Prog. Surf. Sci.* **1992**, *39*, 119−154.

(6) Edwards, D. A.; Wasan, D. T.; Brenner, H. *Interfacial transport processes and technology*; Butterworth-Heinemann: Boston, MA, 1991.

(7) Sonin, A. A.; Bonfillon, A.; Langevin, D. Role of surface elasticity in the drainage of foam films. *Phys. Rev. Lett.* **1993**, *71* (14), 2342−2345.

(8) Prins, A. Surface Stagnant behaviour and its effect on foam and film stability. *Colloids Surf. A* **1999**, *149*, 467−473.

(9) Martin, A. H.; Grolle, K.; Cohen-Stuart, M. A.; Van Vliet, T. Network Forming Properties of Various Proteins Adsorbed at the Air−Water Interface in Relation to Foam Stability. *J. Colloid Interface Sci.* **2002**, *254*, 175−183.

(10) Gandolfo, F. G.; Rosano, H. L. Interbubble Gas Diffusion and the Stability of Foams. *J. Colloid Interface Sci.* **1997**, *194*, 31−36.

(11) Stone, H.; Koehler, S. A.; Hilgenfeldt, S.; Durand, M. Perspectives on foam drainage and the influence of interfacial rheology. *J. Phys: Condens. Matter* **2003**, *15*, S283−S290.

(12) Hemar, Y.; Hocquart, R.; Lequeux, F. Linear shear rheology of incompressible foams. *J. Phys. II Fr.* **1995**, *5*, 37−52.

(13) Buzza, D. M. A.; Lu, C.-Y. D.; Cates, M. E. *J. Phys. II Fr.* **1995**, *5*, 1567−1576.

(14) Mannheimer, R. J.; Schechter, R. S. An improved apparatus and analysis for surface rheological measurements. *J. Colloid Interface Sci.* **1970**, *32* (2), 195−211.

(15) Poskanzer, A. M.; Goodrich, F. C. Surface viscosity of sodium dodecyl sulfate solutions with and without added dodecanol. *J. Phys. Chem.* **1975**, *79* (20), 2122−2126.

(16) Goodrich, F. C.; Allen, L. H.; Poskanzer, A. A new surface viscometer of high sensitivity 1. theory. *J. Colloid Interface Sci.* **1975**, *52* (2), 201−212.

(17) Poskanzer, A.; Goodrich, F. C. A new surface viscometer of high sensitivity 2. experiments with stearic acid monolayers. *J. Colloid Interface Sci.* **1975**, *52* (2), 213−221.

(18) Zacri, C.; Renault, A.; Berge, B. Comparison between macroscopic and microscopic measurements of the shear elastic constant of alcohol monolayers at the air−water interface. *Physica B* **1998**, *248*, 208−210.

(19) Sato, N.; Ito, S.; Yamamoto, M. Molecular weight depedance of shear viscosity of a polymer monolayer: evidence for the lack of chain entenglement in the two-dimensional plane. *Macromolecules* **1998**, *31*, 2673−2675.

(20) Brooks, C.; Fuller, G. G.; Frank, C. W.; Robertson, C. R. An interfacial stress rheometer to study rheologcal transitions in monolayers at the air−water interface. *Langmuir* **1999**, *15*, 2450−2459.

(21) Ding J.; Warriner, H. E.; Zasadzinski, J. A. Magnetic Needle Viscometer for Langmuir Monolayers. *Langmuir* **2002**, *18*, 2800−2806.

(22) Sachetti, M.; Yu, H.; Zografi, G. Hydrodynamic coupling of monolayers with subphase. *J. Chem. Phys.* **1993**, *99* (1), 563−566.

(23) Petkov, J. T.; Danov, K. D.; Denkov, N. D. Precise method for measuring the shear surface viscosity of surfactant monolayers. *Langmuir* **1996**, *12*, 2650−2653.

(24) Regismond, S. T. A.; Gracie, K. D.; Winnik, F. M.; Goddard, E. D. Polymer−surfactant complexes at the air−water interface detected by a simple measure of surface viscoelasticity. *Langmuir* **1997**, *13*, 5558−5562.

(25) Regismond, S. T. A.; Winnik, F. M.; Goddard, E. D. Surface viscoelasticity in mixed polycation anionic surfactant systems studied by a simple test. *Colloids Surf. A* **1996**, *119*, 221−228.

(26) Stenvot, C.; Langevin, D. Study of viscoelasticity of soluble monolayers using analysis of propagation of excited capillary waves. *Langmuir* **1988**, *4*, 1179−1183.

(27) Monroy, F.; Giermanska Kahn, J.; Langevin, D. Dilational viscoelasticity of surfactant monolayers (capillary waves). *Colloids Surf. A* **1998**, *143*, 251−260.

(28) Hard, S.; Neuman, R. D. Viscoelasticity of monomolecular films: a laser light-scattering study. *J. Colloid Interface Sci.* **1987**, *120* (1), 15−29,.

(29) Miller, R.; Sedev, R.; Schano, K. H.; Ng, C.; Neumann, A. W. "Relaxation of adsorption layers at solution/air interfaces using axisymmetric drop-shape analysis. *Colloids Surf.* **1993**, *69*, 209−216.

(30) Loglio, G.; Pandolfini, P.; Miller, R.; Makivski, A. V.; Ravera, F.; Ferrari, M.; Liggieri, L. Drop and Bubble shape analysis as a tool for dilatational rheological studies of interracial layers. In *Novel methods to study interfacial layers*; Möbius, D., Miller, R., Eds.; Studies in interface sciences, Vol. 11; Elsevier: Amsterdam, 2001; pp 439−484.

(31) Kovalchuk, J.; Krägel, E. V.; Aksenenko, G.; Loglio; Liggieri, L. Oscillating bubble and drop techniques. In *Novel Methods to Study Interfacial Layers*; Möbius, D., Miller, R., Eds.; Studies in Interface Science Vol. 11; Elsevier: Amsterdam, 2001; pp 485−517.

(32) Miller, R.; Wustneck, R.; Kragel, J.; Kretzschmar, G. Dilational and shear rheology of adsorption layers at liquid interfaces. *Colloids Surf. A* **1996**, *111*, 75−118.

(33) Freer, E. M.; Yim, K. S.; Fuller, G. G.; Radke, C. J. Interfacial rheology of globular and flexible proteins at hexadecane/water interface: comparison of shear and dilatation deformation. *J. Phys. Chem. B*, in press.

(34) Graham, D. E.; Phillips, M. C. Proteins at liquid interfaces. IV. Dilatational properties, V. Shear properties. *J. Colloid Interface Sci.* **1980**, *76*, No. 1, 227−250.

(35) Petkov, J. T.; Gurkov, T. D.; Campbell, J. T.; Borwankar, T. D. Dilatational and shear elasticity of gellike protein layers on air−water interface. *Langmuir* **2000**, *16*, 3703−3711.

(36) Murray, B. S.; Ventura, A.; Lallemant, C. Dilatational rheology of protein + non ionic surfactant films at air−water and oil−water interfaces. *Colloids Surf. A* **1998**, *143*, 211−219.

(37) Pezennec, S.; Gauthier, F.; Alonso, C.; Graner, F.; Croguennec, T.; Brule, G.; Renault, A. The protein net electric charge determines the surface rheological properties of ovalbumin at the air−water interface. *Food Hydrocolloids* **2000**, *14*, 463−472,.

(38) Dickinson, E. Adsorbed protein layers at fluid interfaces: interactions, structure and surface rheology. *Colloids Surf. B* **1999**, *15*, 161−176.

(39) Benjamins, J.; Lucassen-Reynder, E. H. Surface dilational rheology of proteins adsorbed at air−water and oil−water interfaces. In *Proteins at liquid interfaces*; Möbius, D., Miller, R., Eds.; Elsevier Science B.V.: Amsterdam, 1998.

(40) Hambarddzumyan, A.; Aguié-Béghin, V.; Daoud, M.; Douillard, R. β casein and symmetrical triblock copolymer (PEO−PPO−PEO and PPO−PEO−PPO) surface properties at the air−water interface. *Langmuir* **2004**, *20*, 756−763.

(41) Pereira, L. G.; Théodoly, O.; Blanch, H. W.; Radke, C. J. Dilational rheology of BSA conformers at the air−water interface. *Langmuir* **2003**, *19*, 2349−2356.

(42) Bhattacharyya, A.; Monroy, F.; Langevin, D.; Argillier, J.-F. Surface Rheology and Foam Stability of Mixed Surfactant−Polyelectrolyte Solutions. *Langmuir* **2000**, *16*, 8727−8732.

(43) Ritacco, H.; Kurlat, D.; Langevin, D. Properties of Aqueous Solutions of Polyelectrolyte and Surfactants of Opposite Charge: Surface tension, Surface Rheology and Electrical Birefringence Studies. *J. Phys. Chem. B* **2003**, *107*, 9146−9158.

(44) Monteux, C.; Williams, C. E.; Meunier, J.; Anthony, O.; Bergeron, V.; Adsorption of oppositely charged Polyelectrolyte/Surfactant Complexes at the Air/Water Interface: Formation of Interfacial Microgels. *Langmuir* **2004**, *20*, 57−63.

(45) Monteux, C.; Williams, C. E.; Bergeron, V. Interfacial microgels formed by oppositely charged polyelectrolyte-surfactants. Part II: influence of surfactant chain length and surfactant−polyelectrolyte ratio. *Langmuir*, in press.

(46) Bergeron, V.; Langevin, D.; Asnacios, A. Thin Film Forces in Foam Films Containing Anionic Polyelectrolyte and Charged Surfactants. *Langmuir* **1996**, *12*, 1550−1556.

(47) Monteux, C.; Llauro, M−F.; Baigl, D.; Williams, C. E.; Anthony, O.; Bergeron, V. Interfacial microgels formed by oppositely charged polyelectrolyte-surfactants. 1. Influence of polyelectrolyte molecular weight. *Langmuir*, in press.

(48) Baigl, D.; Seery, T. A. P.; Williams, C. E. Preparation and Characterization of Hydrosoluble, Partially Charged Poly(styrenesulfonate)s of various Controlled Charge Fractions and Chain lengths. *Macromolecules* **2002**, *35*, 2318−2326.

(49) Rotenberg, V.; Bruvka, L.; Neumann, A. W. Determination of Surface Tension and contact Angle from the Shapes of Axisymmetric Fluid Interfaces. *J. Colloid Interface Sci.* **1983**, *93*, 169−183.

(50) Taylor D. J. F.; Thomas, R. K.; Penfold, J. The Adsorption of Oppositely Charged Polyelectrolyte/Surfactant Mixtures: Neutron Reflection from Dodecyl Trimethylammonium Bromide and Sodium Poly(styrene sulfonate) at the Air/Water Interface. *Langmuir* **2002**, *18*, 4748−4757.

(51) Bantchev, G. B.; Schwartz, D. K. Surface Shear Rheology of b-casein Layers at the Air−Solution Interface: Formation of a Two-Dimensional Physical Gel. *Langmuir* **2003**, *19*, 2673−2682.

(52) Winter, H.; Chambon, F. Analysis of linear viscoelasticity of a cross-linking polymer at the gel point. *J. Rheol.* **1986**, *30* (2), 367−382.

(53) Ferry, J. D. *Viscoelastic properties of polymers*, 3rd ed.; John Wiley and Sons: New York, 1980.

(54) Macosko, C. W. *Rheology principles, measurements and applications*; Wiley-VCH: New York, 1993.

(55) Brooks, C. F.; et al. Surface shear rheology of a UV-polymerized lipopolymer layer. *Langmuir* **2002**, *18* (6), 2166−2173.

(56) Naumann, C. A.; Brooks, C. F.; Fuller, G. G.; Lehmann, J.; Ruhe, J.; Knoll, W.; Kuhn, P.; Nuyken, O.; Frank, C. W. Two-dimensionzal Physical Networks of lipopolymers at the air−water interface: correlation of molecular behavior and surface rheological behavior. *Langmuir* **2001**, *17*, 2801−2806.

(57) Naumann, C. A.; Brooks, C. F.; Wiyatno, W.; Knoll, W.; Fuller, G. G.; Frank, C. W. Rheological properties of lipopolymers-phospholipid mixtures at the air−water interface: a novel form of two-dimensional physical gelation. *Macromolecules* **2001**, *34*, 3024−3032.

(58) Guerrini, M. M.; Lochhead, R.; Daly, W. H. Interactions of aminoalkylcarbamoyl cellulose derivatives and sodium dodecyl sulfate. 2. Foam stabilization. *Colloids Surf. A* **1999**, *147*, 67−78.

(59) Ross, S.; Nishioka, G. The relation of foam behaviour to phase separations in polymer solutions. *Colloid Polym. Sci.* **1977**, 255, 560−565.

(60) Ross, S.; Nishioka, G. Foaminess of binary and ternary solutions. *J. Phys. Chem.* **1975**, *79* (15), 1561−1565.

(61) Garrett, P. R.; Davies, J.; Rendall, H. M. An experimental study of the antifoam behavior of mixtures of a hydrocarbon oil and hydrophobic particles. *Colloids Surf. A* **1994**, *85* (2−3), 159−197.

(62) Malzert, A.; Boury, F.; Saulnier, P.; Benoit, J. P.; Proust, J. E. Rheological study of Lysozyme and PEG2000 at the air−water and dichloromethane-methane interfaces under Ramp type or sinusoidal perturbations. *Langmuir* **2002**, *18*, 10248−10254.

(63) Monroy, F.; Rivillon, S.; Ortega, F.; Rubio, R. G. Dilational rheology of Langmuir Polymer Monolayers: Poor-solvent Conditions. *J. Chem. Phys.* **2001**, *115*, No. 1, 530−539.

(64) Noskov, B. A. Dynamic surface elasticity of polymer solutions. *Colloid Polym. Sci.* **1995**, *273*, 263−270.

(65) Noskov, B. A.; Akentiev, A. V.; Bilibin, A. Y.; Zorin, I. M.; Miller, R. Dilational surface viscoelasticity of polymer solutions. *Adv. Colloid Interface Sci.* **200**3, *104*, 245−271.